RSC Advances

ROYAL SOCIETY OF CHEMISTRY

www.rsc.org/advances

Nitric oxide decomposition using atmospheric pressure dielectric barrier discharge reactor with different adsorbents

Xiaolong Tang , Fengyu Gao, Jiangen Wang, Honghong Yi* and Shunzheng Zhao

Department of Environmental Engineering, Civil and Environmental Engineering School, University of Science and Technology Beijing, Beijing, 100083, PR China.

Abstract:

An NO removal rate of 99% was obtained on NaY zeolite at an energy efficiency of 99.4 g NO/kWh using the ADD process.

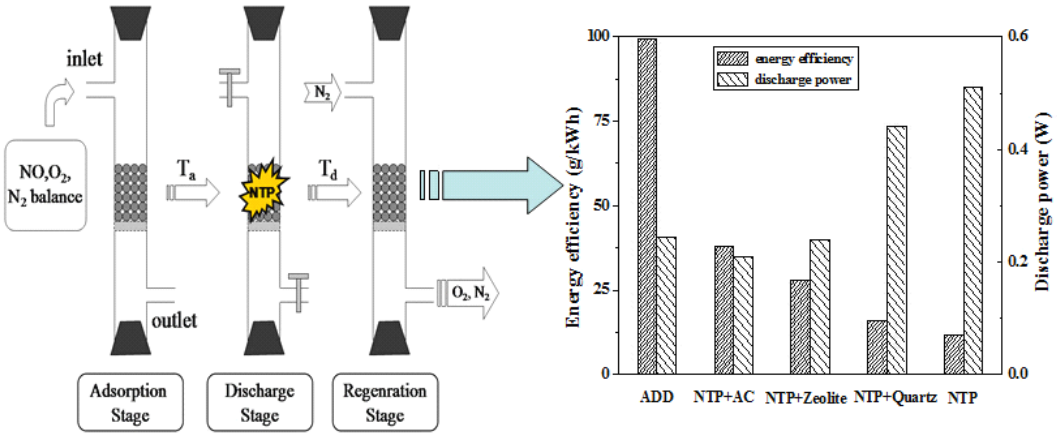

Highlights:

1. NTP was obtained in a self-made coaxial cylinder-type DBD reactor.

2. A cycled adsorption-desorption and decomposition process was investigated.

3. Almost 100% NO removal efficiency and energy efficiency of 99.4 g NO/kWh were achieved.

Nitric oxide decomposition using atmospheric pressure dielectric barrier discharge reactor with different adsorbents

Xiaolong Tang , Fengyu Gao, Jiangen Wang, Honghong Yi* and Shunzheng Zhao

Department of Environmental Engineering, Civil and Environmental Engineering School, University of Science and Technology Beijing, Beijing, 100083, PR China.

* *Corresponding author:* HongHong Yi

Tel./fax:+86 010 62332747. *E-mail address:* yhhtxl@126.com

Abstract: A cycled adsorption–desorption and decomposition process (ADD) for removing NO_x was designed and performed using a dielectric barrier discharge (DBD) reactor filled with NaY zeolite or activated carbon as absorbent at ambient temperature. Simulated flue gas was introduced into the DBD reactor for adsorption (T_a). Non-thermal plasma (NTP) was applied to detach and decompose the adsorbed NO for a specific period (T_d). Some key operating conditions (adsorbent materials, discharge power, T_d, and so on) were investigated to optimize the ADD process, and the effects of H_2O and O_2 were also involved. NO conversion, NO_2 formation, and energy efficiency among different NTP-assisting $DeNO_x$ technologies were compared. The experimental results demonstrated that an NO removal rate of 99% was obtained on NaY zeolite at an energy efficiency of 99.4 g NO/kWh using the ADD process.

Key words: Nitric oxide; NaY zeolite; Desorption, decomposition; Dielectric barrier discharge.

1. Introduction

Nitrogen oxides (NO_x: NO and NO_2) are emitted mainly from stationary combustion and mobile sources. More than 90% of emitted NO_x from stationary sources is in the form of NO [1]. Post-combustion technologies such as selective catalytic reduction (SCR) [2], selective non-catalytic reduction (SNCR) [3], direct decomposition [4], and non-thermal plasma (NTP) [5,6] have been developed to remove NO_x from stationary sources. However, each technology has inherent weaknesses, for instance, the drawbacks are the narrow operating temperature window, ammonia slip for SCR [7,8] and SNCR[9], catalysts poisoning for SCR[10], high energy consumption for decomposition[11] and NTP [6,12].

The most distinctive characteristic of the NTP technology is the ability to induce various chemical reactions at atmospheric pressure and room temperature [5,13]. However, complete removal of NO using NTP alone is difficult because O_2 oxidizes NO to NO_2 [14]. Energy consumption is high for NO reduction using NTP treatment alone. Currently, numerous studies have been performed to overcome these weakness, including investigations about NTP-assisted catalytic reduction [15], NTP-assisted SCR [6,16], NTP combined with non-catalytic pellets [17], different electric discharges [5,18], and geometry of NTP reactor [19]. NO removal efficiency evidently increases, but energy consumption still remains high because the NTP reactor should be operated sustainably during the whole NO treatment process.

NTP desorption has been studied for catalyst/adsorbent regeneration [20], volatile organic compounds (VOCs) removal [21], and NO_x removal [14,22]. Kuroki et al [20] investigated the regeneration of honeycomb zeolite by nonthermal plasma desorption of toluene, and obtained an extremely effective and practical VOC removal process in spite of a regeneration efficiency of approximately 75%. Ogata et al [21] investigated the plasma process combined with adsorption using a zeolite-hybrid reactor for dilute benzene removal to enhance the energy efficiency of the plasma reactor and suppress the formation of byproducts (NOx). Qu et al [22] obtained about 97.8% NOx removal

rate and 0.758 mmol NOx/W·h energy efficiency on 8.5wt.% carbon mixed H-ZSM-5 catalysts by using the combined adsorption-discharge plasma catalytic process for NOx without external heating.

In the present work, we proposed and investigated a high-efficiency method to remove NO using NTP with cycled adsorption–desorption and decomposition (ADD) process [23]. In this study, NaY zeolite and activated carbon (AC) were used as high-efficiency adsorbents and set in the discharge area of the dielectric barrier discharge (DBD) reactor to adsorb a large amount of NO, And them NTP was then applied to detach and decompose the adsorbed NO. Some operating conditions (adsorbent materials, discharge power, T_d, and so on), the effect of H_2O and SO_2, and the comparison of different NTP-assisted $DeNO_x$ technologies were also studied and discussed.

2. Experimental

2.1 NTP desorption and decomposition system.

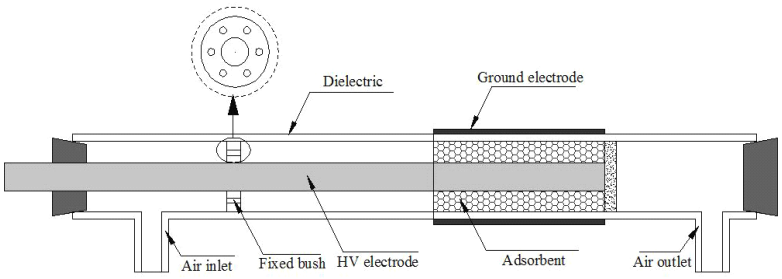

Fig. 1. Dielectric barrier discharge (DBD) reactor

As shown in Fig. 1, NTP was obtained in a coaxial cylinder-type DBD reactor with sinusoidal high voltage power input generated by a plasma generator in the range of 0-30 kV voltage and 5-25 kHz frequency (CTP-2000K, Nanjing Suman Electronics co., LTD, China). The DBD reactor tube composed of quartz with 10mm inner diameter, similar to our previous studies [23,24], which was functioned as dielectric layer. The discharge area between high voltage electrode and ground electrode was

filled with the adsorbents. In this work, the length of discharge area and discharge gap is 50 mm and 3.5 mm, respectively.

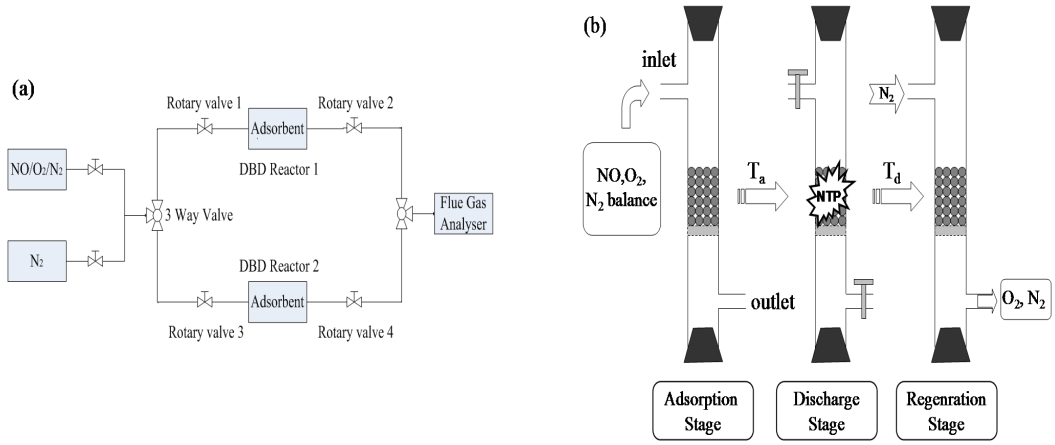

Fig. 2. The experimental flowchart (a) and the schematic of adsorption–desorption and decomposition process (ADD) for NO removal (b).

Fig. 2(a) and (b) presents the experimental flowchart and the schematic of adsorption–desorption and decomposition process (ADD) for NO removal, respectively. There are two parallel DBD reactors filled with adsorbents in the discharge area. Simulated gas containing 500ppm NO, 3vol% O_2, and N_2 (as balance gas) was entered into the DBD reactor 1 for adsorption (T_a), and the clean gas was emitted into the air. After T_a period, high voltage power was applied in the DBD reactor 1 without gas flow (closing rotary valves 1 and 2) to produce NTP. Simultaneously, the path of simulated gas was changed to reactor 2 using the rotary valves for another similar experiment. During the discharge period of reactor 1, the adsorbed NO was desorbed from the adsorbent because of the effects of joule heat and high-energy electron caused by electric discharge. NO was decomposed to N_2 and O_2 through NTP in this stage (T_d). After desorption and decomposition, the adsorbents were regenerated using NTP. The system was operated in a cycled adsorption–desorption and decomposition process. NTP was only produced in the decomposition period (T_d), thus total energy consumption can be reduced significantly by controlling the rate of T_a/T_d.

2.2 Method and On-line analysis.

The voltage applied in the DBD reactor was measured by a high voltage probe (Pintek, HVP-28HF, 1000:1). A non-inductive capacitor (C_m=0.01 μF) was inserted between DBD reactor and the ground electrode, when discharge power (P) of the DBD reactor was detected. The V-Q lissajous method [25] was used to measure the discharge power dissipated in the DBD reactor. Discharge power was calculated using the followed formula:

$$P(W) = f \times A \times C_m \qquad (1)$$

Where f indicates the frequency of applied voltage (kHz); A denotes the area of V-Q lissajous curves.

Energy efficiency (denoted as η, unit is g NO/kWh) is used to compare the energy consumption among the different DBD reactors, it calculated as follows:

$$\eta(\mathrm{g}/kWh) = \frac{3600 \times 30}{22.4 \times 60 \times 1000} \cdot \frac{Q \times T_a \times (NO_{inlet} - NO_{outlet})}{P \times T_d} \qquad \text{or}$$

$$\eta(\mathrm{g}/kWh) = \frac{9}{112} \cdot \frac{Q \times NO_{inlet}}{P} \cdot X_{NO} \cdot \frac{T_a}{T_d} \qquad (2)$$

Where NO_{inlet} and NO_{outlet} are the concentration of NO in the inlet and outlet of the reactor (ppm), respectively; Q denotes the flow rate of simulated gas (L/min);

The concentration of NO and NO_2 were detected by flue gas analyzer (Kane, KM9106). The NO conversion of NTP assisted DeNO$_x$ was obtained by the followed equation:

$$X_{NO}\ (\%) = \frac{NO_{inlet} - NO_{outlet}}{NO_{inlet}} \times 100 \qquad (3)$$

The NO removal efficiency of ADD system was obtained by the followed equation:

$$NO_{removal}(\%) = \left(1 - \frac{V' + V''}{V}\right) \times 100 = \left(1 - \frac{\int_0^{T_a} NO_{outlet}\,dt + \int_0^{T_D} NO_{outlet}\,dt}{NO_{inlet} \times T_a}\right) \times 100 \qquad (4)$$

Where V is the volume of NO supplied to the reactor during the adsorption stage (T_a=30min); V' is the volume of NO emitted from the DBD reactor during the

adsorption stage; V'' is the volume of NO emitted from the DBD reactor during the desorption and decomposition stage; T_D is the period of desorption and decomposition stage with gas flow.

2.3 Adsorbents preparation.

The commercial coconut shell based activated carbon (AC) and NaY zeolite were from the WEISHIMEI science and Technology Ltd and Nankai University (Tianjin, China), respectively. The details of the BET-surface area, pore volume, and pore size of AC and NaY adsorbents were summarized in Table 1, based on our previous research[26,27]. Besides, the saturated adsorption capacity calculated by the results of NO adsorption and TPD-desorption was about 0.30 mmol NO/g-NaY and 0.21mmol NO/g-AC, respectively. The adsorbents were crushed and sieved to 0.25-0.38 mm size, and washed 3 times with distilled water. Then the adsorbents were dried for 5-6 hours at 100℃ in the drying oven. At the beginning of the experiments, adsorbents (3.6 ml in each test) were prepared by NTP under an atmosphere of N_2 for 30 min. The NTP was obtained in the DBD reactor operated at 5.5 kV and 8.9 kHz.

Table 1 Characterization of the adsorbents.

Samples	BET-surface area (m^2/g)	Pore volume (cm^3/g)	Average pore diameter (nm)	Adsorption capacity of NO (mmol/g) *
AC[26]	606	0.35	1.11	0.21
NaY[27]	542	0.38	3.29	0.30

* The saturated adsorption capacity was calculated by the results of NO adsorption and TPD-desorption.

3 Results and discussion

3.1 Adsorption performance of adsorbent with NTP.

It is well known that the adsorption process has a significant influence on the NO removal efficiency of NTP-assisted reduction [22]. Adsorbents with a significant adsorption capacity of NO can prolong the retention time of NO in the NTP zone,

which could improve the NO removal efficiency and reduce the energy consumption [28]. However, if the discharge power is not enough to detach the adsorbed NO, a lot of NO would be remained on the adsorbents. The adsorption-decomposition equilibrium of reactions in NTP is greatly influenced by the operating conditions of NTP reactor. The most significant operating condition is the discharge power, which is mainly varied with discharge voltage applied on the DBD reactor. Therefore, for NTP desorption, it is necessary to select an appropriate discharge power (voltage) to make sure that NO is completely desorbed by NTP instead of adsorbed on adsorbents. As shown in Fig. 3, adsorption performances of NaY zeolite and AC under different discharge voltage were investigated, respectively. 500 ppm NO with a flow rate of 0.2 L/min was entered into the DBD reactor, and the reactor was operated continuously at 8.9 kHz 15 min for each voltage.

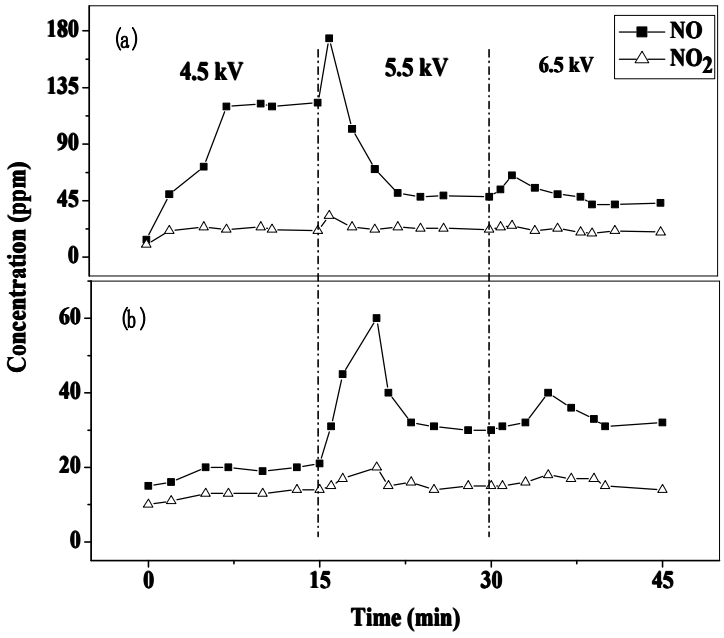

Fig. 3. Effect of voltage on the outlet NOx concentration with NaY zeolite (a) and AC (b) as adsorbents, Conditions: the total flow rate was 0.2L/min; frequency applied on the DBD reactor was 8.9 kHz; operated at room temperature.

Fig. 3(a) shows that the outlet NO concentration (NO_{outlet}) was maintained at 120, 50, and 46 ppm after few minutes of reaction at specified voltages (4.5, 5.5, and

6.5 kV, respectively). The NO_{outlet} increased from 20 ppm to 120 ppm after operation at 4.5 kV. The discharge power of the NTP reactor at 4.5 kV was 0.11 W, which was insufficient to desorb and reduce more NO gas from the adsorbent; thus, the abundantly adsorbed NO remained on NaY zeolite. The NO_{outlet} showed a sudden increasing trend when the voltage was increased from 4.5 kV to 5.5 kV. However, this phenomenon was not observed when the voltage was further increased. The NTP desorption is related to the effect of electrons, ions, radicals, etc, which increased with the discharge power augmented by the increase of input voltage [20,21]. The result presented in Fig. 3(b) shows that the NO_{outlet} followed a trend similar to that in Fig. 3(a). The NO_{outlet} increased from 10 ppm to 24 ppm after the DBD reactor was operated at 4.5 kV for 15 min. The amount of NO remaining on the absorbents decreased with increasing discharge power (voltage), but the augmented NO_{outlet} was not evident when the voltage increased from 5.5 kV to 6.5 kV. It means that the applied voltage setted at 5.5 kV is reasonable, economic and energy-efficient for NO abatement.

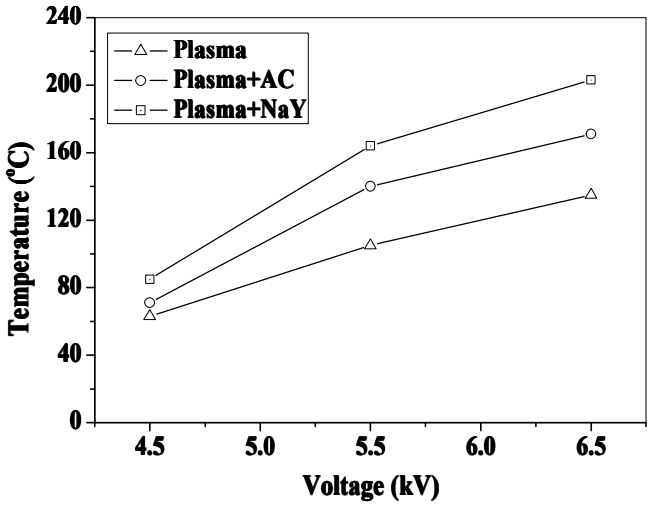

Fig. 4. Effect of voltage on temperature of DBD reactor.

Fig. 4 shows that the temperature of DBD reactor was increased from 86℃ to 164℃ after a few minute of reaction at 5.5kV. The desorption of NO from adsorbents happened with the rise of temperature caused by the NTP discharge. NO was mainly

decomposed to N_2 and O_2 with the augment of discharge power, and the amounts of NO remained on adsorbents was decreased. The removal efficiency of NTP assisted reduction would not be infinitely improved by increasing discharge power. As shown in Figure 3a, the NO_{outlet} of 5.5 kV and 6.5 kV was 50 ppm and 46 ppm, respectively.

3.2 NTP desorption and decomposition of NO removal

3.2.1 Effect of T_d on NO removal efficiency.

In this section, NaY Zeolite and AC were used as adsorbent material to adsorb NO, respectively. The NO concentration and flow rate were set as 500 ppm and 0.2 L/min, respectively. The NO_{outlet} was less than 20 ppm during the period of adsorption stage. The adsorption performance of NaY zeolite and AC in NTP could be neglected at 5.5 kV, so the applied voltage was set at 5.5 kV. Because NTP was not applied in the adsorption process, the energy consumption would be decreased with the ratio of T_d/T_d increase. Therefore, Effects of T_a and T_d on NTP adsorption-desorption and decomposition performances were investigated.

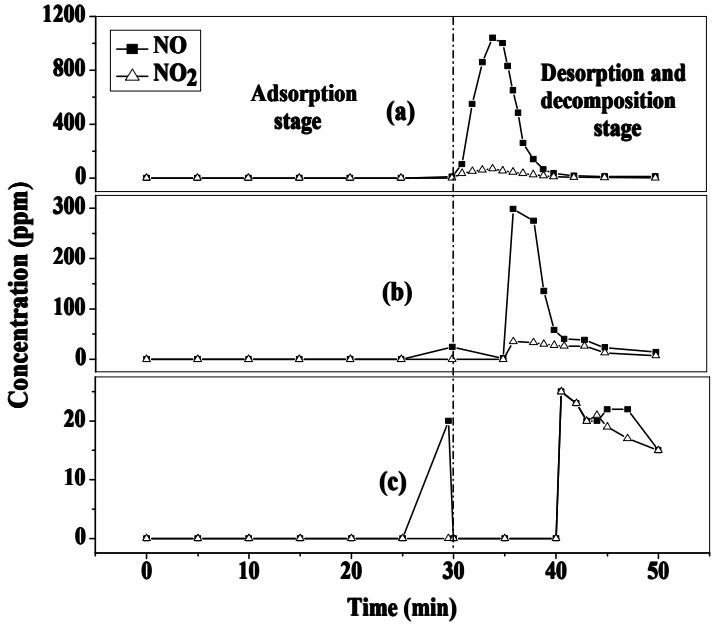

Fig. 5. NTP desorption and decomposition for NO reduction with NaY zeolite as absorbent (a: T_d= 0 min, b: T_d= 5 min, c: T_d= 10 min), the discharge power of DBD reactor was 0.24 W, space velocity of adsorbent was 3360 h^{-1}.

As shown in Fig. 5(a), 500 ppm NO was introduced into the DBD reactor for 30 min and all NO was adsorbed onto the NaY zeolite. N_2 with a flow rate of 0.2 L/min was introduced into the DBD reactor instead of the simulated gas, and then NTP was applied simultaneously. The concentration of the emitted NO from the DBD reactor increased to 1040 ppm after few minutes of reaction at 5.5 kV. The NO removal efficiency was about 70%. The results presented in Fig. 5(b) show that the maximum concentration of the emitted NO was 298 ppm when the first 5 min of NTP desorption and decomposition process was without gas flow (T_d = 5 min). In this condition, the NO removal efficiency was improved to 92%. The NO removal efficiency increased to 99% when T_d was further increased (Fig. 5(c), T_d= 10 min). In a given discharge power (voltage), the NO removal efficiency can be increased by extending T_d.

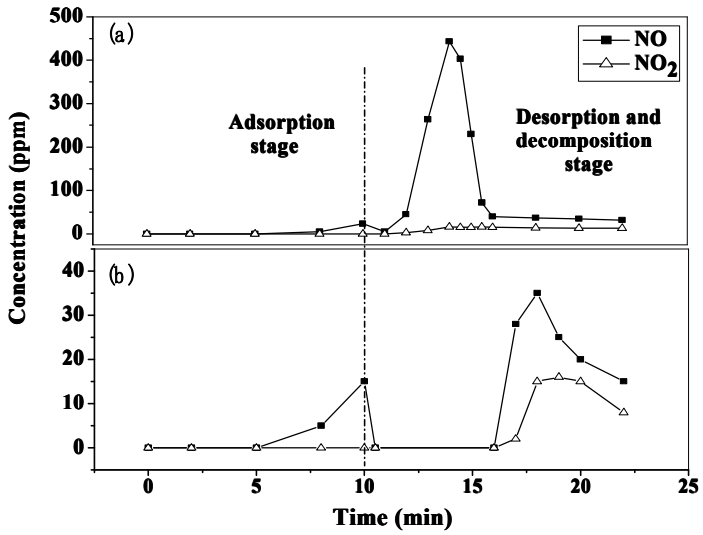

Fig. 6. NTP desorption and decomposition for NO reduction with AC as absorbent (a: T_d= 0 min; b: T_d= 6 min), the discharge power of DBD reactor was 0.20 W, space velocity of adsorbent was 3360 h^{-1}.

Adsorbent materials have significant function on the ADD process for NO reduction. An appropriate adsorbent material prolongs the adsorption period (T_a) but also reduces the discharge power of the DBD reactor. Similar regularity was observed during the NTP desorption and decomposition process with AC as the adsorbent, as

shown in Fig. 6. The period of adsorption stage was 10 min, and T_d for the NO desorption and decomposition was 6 min. The discharge power of the DBD reactor with AC (0.20 W) was lower than that of the DBD reactor with NaY zeolite (0.24 W). However, the ratio of T_a/T_d = 3 for the DBD reactor with zeolite was higher than that of the DBD reactor with AC (T_a/T_d = 1.67). Therefore, NaY zeolite is more appropriate for the NTP adsorption and decomposition. The correlation between Ta/Td and NO removal efficiency, and energy efficiency were presented by changing the time of the decomposition period (T_d), and summarized in Table 2. In the ADD system, the NO removal efficiency was increased with T_d increase, but the energy efficiency decreased. As T_d was 10 min, 99% of NO removal efficiency with an energy efficiency of 99.4 g NO/kWh was obtained. But, the energy efficiency decreased rapidly as T_d was increased to 15 min. Therefor, T_d = 10 min is reasonable, economic and energy-efficient for NO abatement in this study.

Table 2 The correlation between T_a/T_d and NO removal efficiency, and energy efficiency (NaY zeolite absorbent)

	Time of the decomposition period (T_d, min, T_a=30 min)				
	0 *	5	10	15	30
T_a/T_d	—	6	3	2	1
X_{NO} (%)	70	92	99	100	100
η (g/kWh)	35.2	184.8	99.4	66.9	33.6

* NTP was used with the gas flow for 20min.

3.2.2. Effect of O_2 and H_2O on the NO removal efficiency in the ADD system.

The results presented in Fig. 7 show that the NO removal efficiency of the ADD system was enhanced when the O_2 concentration was increased. The concentration of O_2 mainly affected the adsorption of NO in the first stage (T_a), but had minimal effect on the desorption and decomposition of NO in the second stage. This finding can be attributed to the absence of gas flow in the closed system. The adsorption performance of NaY for NO was enhanced by increasing the O_2 concentration,

particularly when the O_2 fraction was lower than 3%. When the concentration of O_2 increased by more than 3%, the NO gas is completely absorbed onto the NaY zeolite during the adsorption stage (T_a) and the NO removal efficiency is 99%.

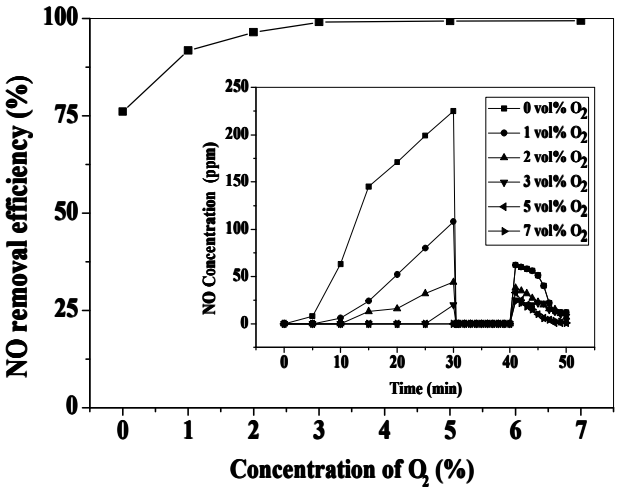

Fig. 7. Effect of O_2 concentration on the NO removal efficiency. Conditions: NaY zeolite as adsorbent, T_d = 10 min;NO = 500 ppm, Q = 0.2 L/min; V = 5.5 kV, P = 0.24 W.

It clearly demonstrates the presence of O_2 in the flue gas is essential for achieving high NO adsorption for NaY. Based on the reports by Xing [29] and Yang [30], it can postulate that NO is first oxidized to NO_2 (ads) by the adsorbed O2 on the active site of the NaY following the surface reactions below [31]:

$$NO \xrightarrow{O_2} NO_2 \xleftarrow{e^- \text{ from } Na^+ \text{ zeolite}} NO_2^- \qquad (5)$$

Fig. 8(a) shows that the NO removal efficiency decreased with the increasing H_2O concentration, and the adsorption and desorption–decomposition of NO were affected by H_2O concentration. The adsorption performance of NaY for NO decreased with the increasing H_2O concentration, significantly decreased with low H_2O gas. However, the effect was not apparent because H_2O concentration increased to 10% from 8%. Remarkably, the outlet concentration of NO and NO_2 in the NTP process reached the maximum during the increase of H_2O concentration. When the concentration of H_2O increased from 0 to 5%, the outlet concentration of NO

gradually increased and obtained the maximum (166 ppm) at 5% H_2O, but decreased when the H_2O concentration was further increased. The outlet concentration of NO_2 increased initially, and then decreased with the increasing H_2O concentration, as shown in Fig. 8(b).

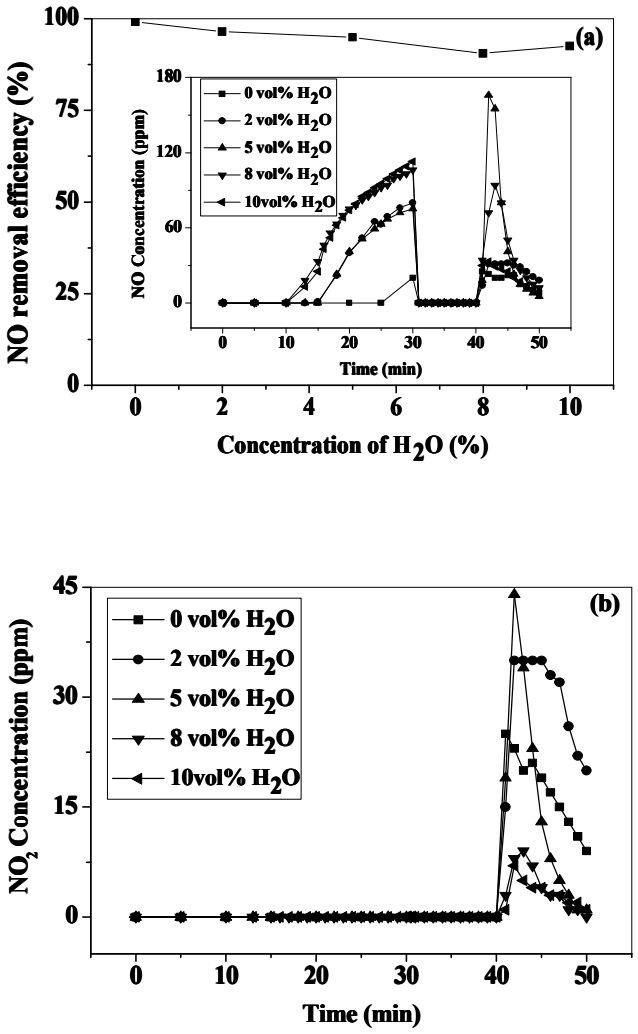

Fig. 8. Effect of H_2O concentration on the NO removal efficiency. Conditions: NaY zeolite as adsorbent, T_d = 10 min;NO = 500 ppm, Q = 0.2 L/min; V = 5.5 kV, P = 0.24 W.

H_2O can be desorbed, activated, and ionized to active radicals (O, OH, HO_2, and so on) through the effect of high-energy electron. A higher H_2O concentration results in more active radicals ionized by H_2O gas during T_d in the closed reactor. NO can be

oxidized to NO_2 by the active radicals (O and HO_2) ionized by H_2O [32], thus the NO_2 concentration increases. However, the concentration of NO and NO_2 decreased when the H_2O concentration was further increased because more active radicals were produced by NTP; thus, NO and NO_2 will be converted to HNO_2 and HNO_3 through the reaction with OH and HO_2 radicals [33].

3.2.3. Reaction process of ADD.

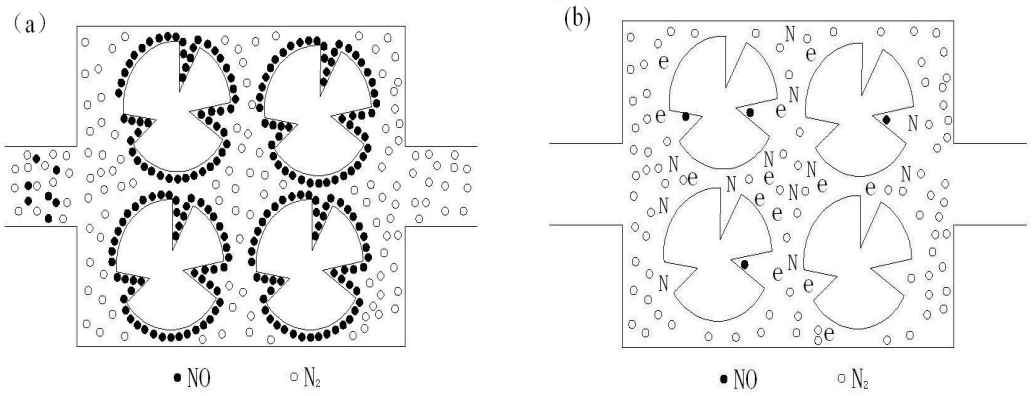

Fig. 9. Schematic of NTP desorption and decomposition for NO removal (a: adsorption stage, b: desorption and decomposition stage).

Fig. 9 shows the theoretical schematics of adsorption–desorption and decomposition for NO reduction using NaY zeolite adsorbent. The simulated gas, including NO, was first entered into the DBD reactor. The NO molecules were adsorbed onto the NaY zeolite pellets, and clean gas was exhausted into the environment. The NO_{outlet} was lower than 20 ppm during the adsorption process. After adsorption (T_a = 30 min), the DBD reactor was operated at 5.5 kV without gas flow. With the NTP production in DBD reactor, the adsorbed NO was desorbed and decomposed by NTP. After the desorption and decomposition process, NaY zeolite was regenerated because of NO desorption. The main reason for NO desorption was the effects of the joule heat and high-energy electron during the NTP process. Sadat et al [34,35] reported that highly reactive species and the joule heat are generated in dielectric barrier discharges (DBD) by using electrode temperatures measurements and an unsteady lumped thermal model, and that the heat will be lost by conduction

across the gas layer and the composite envelope of the reactor. Besides, discharging type changed from the streamers in air alone to the streamers along the insulator surfaces when the adsorbents were introduced in the NTP reactor, indicating that the NTP process occurred on the insulator surface [17]. By the reactor temperature measurements, the surface temperature of the DBD reactor increased to 164 ° C on NaY-ADD system in this study.

Besides, the concentration of N_2O was detected by the Extrel MAX300, the results showed that the N_2O concentration was less than 15ppm. (Conditions: NaY zeolite as absorbent, NO = 500 ppm, Q = 0.2 L/min; V = 4.5, 5.5, and 6.5 kV, respectively.). It can be seen from Fig. 5, the concentration of NO_2 (mainly from the oxidation of NO) was very small (less than 20ppm) due to the low concentration of active radical [O] without gas flow in the second step of ADD process. It was well known that N_2O was mainly generated from the reaction of NO_2 and N radical, and the low concentration N_2O will be quickly decomposition [22]. Therefor, the N_2O concentration was so low that it can be ignored in this study. Besides, the O_3 concentration was not detected by the rapid detector of ozone.

NO would be mainly decomposed to N_2 and O_2 using atomic nitrogen species produced from the residual N_2 during the adsorption and decomposition stage. The main process can be demonstrated through the following equations [36,37,38,22]:

$$e + N_2 \longrightarrow e + N(^4S) + N(^2D) \qquad (6)$$

$$N(^4S) + NO + M \longrightarrow M + N_2 + O \qquad (7)$$

$$N(^4S) + NO_2 \longrightarrow O(^3P) + N_2O \qquad (8)$$

Where M is NaY zeolite.

Considering that the discharge streamers of the DBD reactor with adsorbent were transmitted along the insulator surfaces, the reaction mainly occurred on the surface of NaY zeolite. The amount of O_2 in the system was low during desorption and decomposition stage, but the concentration ratio of NO to O_2 was higher than that

in the pre-existing systems. NTP is mainly formed through the effects of high-energy electrons with N_2 molecules, indicating that $N(^4S)$ is the main species on the NaY zeolite surface that reacts with NO [36,37].

3.2.4. Repetition. Two parallel DBD reactors filled with adsorbents were set in the ADD system, as shown in Figs. 1 and 2. About 500 ppm NO was entered into one of the DBD reactors (R1) for adsorption, and purified gas was emitted into air. The NO_{outlet} was maintained below 20 ppm during the adsorption process. After the adsorption period, the simulated gas was entered into another DBD reactor (R2). Simultaneously, high voltage power was applied in the DBD reactor R1 without gas flow to produce NTP. Fig. 10 shows the repetition results of adsorption–desorption and decomposition for NO removal. The adsorption period for each DBD reactor was 30 min. After adsorption, the DBD reactor was operated at 5.5 kV for 10 min to detach and decompose the adsorbed NO. After this stage, the reactor was cooled for 20 min. Fig. 10 presented that the NO_{outlet} of the system was approximately 0 ppm at the adsorption stage. The NO_{outlet} of desorption and decomposition stage was 0 ppm because NTP was produced through the DBD reactor without gas flow.

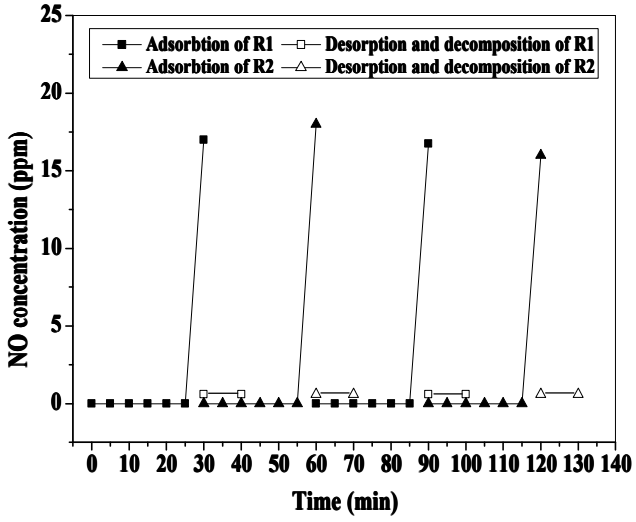

Fig. 10 Adsorption-desorption and decomposition of NO reduction with NaY zeolite, conditions: NO = 500 ppm, Q = 0.2 L/min; V = 5.5 kV, P = 0.24 W.

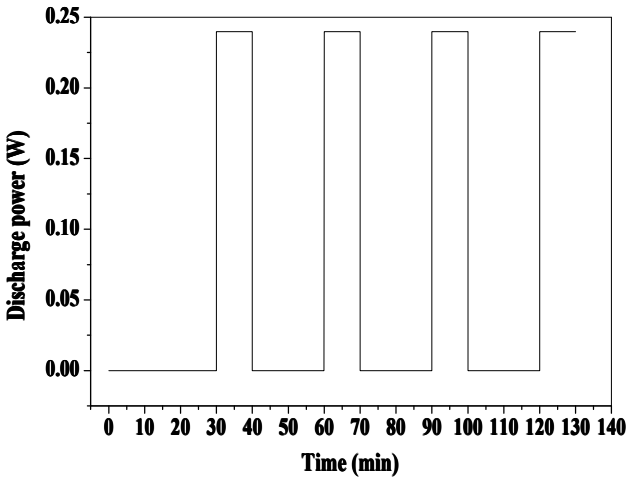

Fig. 11 Discharge power of ADD system.

Fig. 11 shows that discharge power was only consumed during desorption and decomposition process. Power consumption decreased to 33% (T_d/T_a) of the NTP-assisted system. Therefore, long adsorption period and short NTP period were necessary to obtain higher energy efficiency in the ADD system.

3.3. Comparison of different NTP technologies for NO reduction.

Compared with other NO reduction technologies, NTP can be ignited and performed at room temperature. However, the major disadvantages of NTP technology are energy efficiency and production selectivity, which should be further improved. Three other NTP technologies (NO direct decomposition using NTP alone, NTP-assisted catalytic reduction of NO, and packed-bed NTP reactor for NO reduction) were studied to compare the NO reduction performance of different NTP technologies. In this section, two kinds of adsorbents (NaY zeolite and AC) were used for NTP-assisted catalytic reduction of NO. The packed-bed reactor was constructed through packing the non-catalytic dielectric pellets inside the discharge area of the DBD reactor. The typical materials of the non-catalytic dielectric pellets include glass, quartz, ceramic, and ferroelectrics. Quartz pellets with a diameter of 1.5 mm were used in this experiment, and the dielectric constant of quartz was within the range of 4 to 7 mm. The discharge area of the DBD reactors was the same. The NTP reactor for

all experiments in this section was operated at 5.5 kV, whereas frequency was set at 8.6 kHz to 8.9 kHz.

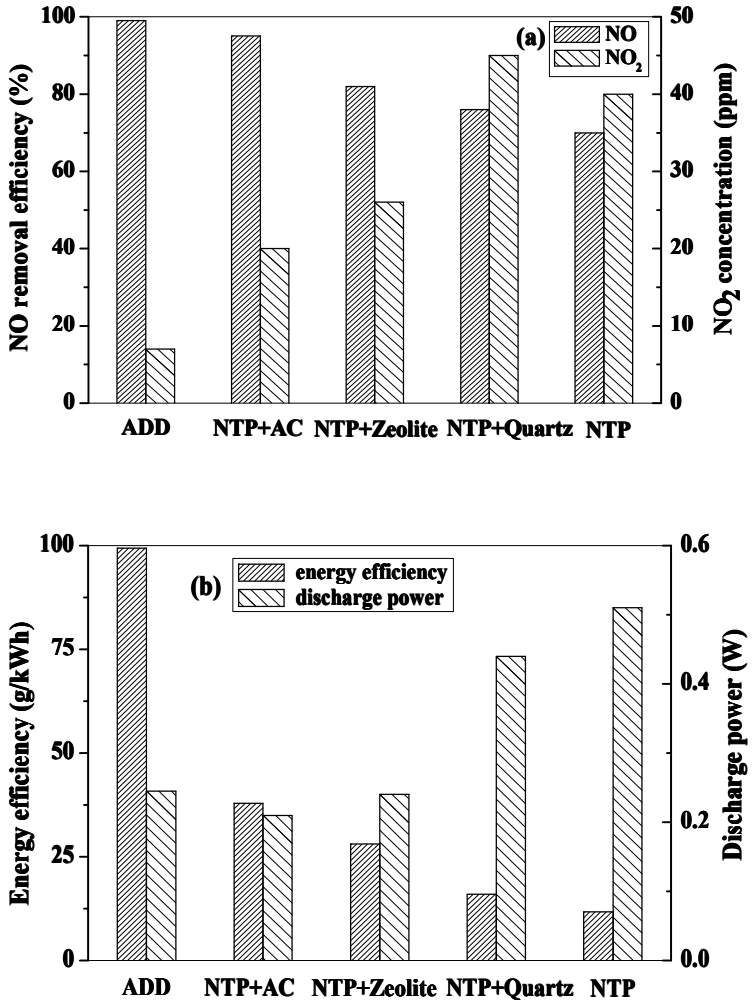

Fig. 12. NO reduction of different NTP technologies at the voltage of 5.5 kV ((a): NO removal efficiency and concentration of NO_2 formation; (b) energy efficiency and discharge power.)

The NO conversion in the NTP alone was 72% with 40 ppm NO_2 formation, as shown in Fig. 12. However, the energy efficiency of the NTP technology was lower than 12 g NO/kWh and can consume more energy to further enhance the NO removal efficiency. The results presented in Fig. 12(a) provide the NO conversion and the amount of NO_2 formation of different NTP methods. The NO conversion was in the following sequence: Desorption and decomposition > NTP + AC > NTP + NaY

zeolite > NTP + Quartz > NTP. In this experiment, NO was mainly decomposed to N_2 and O_2. However, low quantity NO_2 formation was produced in the presence of O_2. Fig. 12(a) also shows that the amount of NO_2 formation for the packed-bed reactor was higher than that of the other NTP methods, even in NTP alone for NO reduction. The major characteristic of the packed-bed reactor was the presence of contact points between pellets, which will enhance the electric field strength. The reaction between the pellets of the packed-bed reactor was more intense, but the direction of the reaction was uncontrollable. Therefore, the NO conversion of the packed-bed DBD reactor was higher than that of the NTP, but the amount of NO_2 formation was higher than that of the NTP alone. The packed-bed DBD reactor can achieve higher electric field and lower discharge power than the conventional DBD reactor. Thus, using non-catalytic dielectric pellets can enhance the electric strength between the pellets and NO conversion, but the control of the by-product for this method was not satisfactory.

The results presented in Fig. 12 indicate that the NTP-assisted catalytic reduction of NO is a technology characterized by high NO conversion, lower by-product, and high-energy efficiency compared with NTP alone and packed-bed DBD reactor. However, the flow rate of the industrial NO emissions was high and their concentration was low (in ppm levels), which will increase the total consumption caused by the size of control system and energy efficiency. In the NO reduction using adsorption–desorption and decomposition technology, the NO removal efficiency was approximately 100%, with an energy efficiency of 99.4 g NO/kWh but without the formation of NO_2. The discharge power of the NTP reactor between the NTP-assisted catalytic reduction of NO and NTP desorption and decomposition was the same when the voltage applied on DBD reactor was the same. However, the energy efficiency of ADD was the highest because no energy was consumed in the adsorption stage.

4. Conclusions

In this paper, a cycled ADD system using absorbents (activated carbon and NaY zeolite) was investigated to reduce NO using NTP. NTP was operated without gas flow, which can prevent the NO emission from the DBD reactor. The NO removal efficiency was approximately 100% at an energy efficiency of 99.4 g NO/kWh. This process can suppress the NO_2 formation because the reaction occurs on the NaY zeolite surface. Compared with the common NTP-assisting $DeNO_x$ technologies, the total power used to decompose NO using the ADD process was lower on order of magnitude because the NTP was not applied during the adsorption process (T_a). Further energy decrease would be achieved when the ratio of T_a/T_d increased, which mainly depends on the adsorbent material, discharge power, and optimum T_d for NO desorption and decomposition.

Acknowledgments

This work was financially supported by National Natural Science Foundation of China (20907018, 21177051).

References

1 J. M. Hao, H. Z. Tian and Y. Q. Lu, *Environ. Sci. Technol.*, 2002, **36**, 552.

2 D. S. Zhang, L. Zhang, C. Fang, R. H. Gao, Y. L. Qian, L. Y. Shi, and J. P. Zhang, *RSC Adv.*, 2013, **3**, 8811.

3 L. Gasnot, D. Q. Dao and J. F. Pauwels, *Energy Fuels*, 2012, **26**, 2837.

4 Y. Yokomichia, T. Yamabe, T. Kakumotoc, O. Okadac, H. Ishikawad, Y. Nakamurad, H. Kimurae and I. Yasudaf, *Appl. Catal., B*, 2000, **28**, 1.

5 G. B. Sretenovi, *J. Hazard. Mater.*, 2011, **185**, 1280.

6 H. Wang, Q. Q. Yu, T. Liu, L. P. Xiao and X. M. Zheng, *RSC Adv.*, 2012, **2**, 5094.

7 M. Kleemann, M. Elsener, M. Koebel, A. Wokaun, *Appl. Catal., B*, 2000, **27**, 231.

8 Y. G. Zhao, J. Hu, L. Hua, S. J. Shuai, J. X. Wang, *Ind. Eng. Chem. Res.*, 2011, **50**, 11863.

9 H. Xu, L. D. Smoot, *Energy Fuels*, 1999, **13**, 411.

10 O. Kröcher, M. Elsener, *Appl. Catal., B*, 2008, **77**, 215.

11 S. Roy, M. S. Hegde, G. Madras, *Appl. Energy*, 2009, **86**, 2283.

12 J. L. Hueso, A. R. Gonalez-Elipe, J. Cotrino, A. Caballero, *J. Phys. Chem. A*, 2007, **111**, 1057.

13 U. Kogelschatz, *Plasma Chem. Plasma Process.*, 2003, **23**, 1.

14 M. Okubo, M. Inoue and T. Kuroki, *IEEE T. Ind. Appl.*, 2005, **41**, 891.

15 J. H. Kwak, J. Szanyi and C. H. F. Peden, *Catal. Today*, 2004, **89**, 135.

16 J. H. Li, R. Ke, W. Li and J. M. Hao, *Catal. Today*, 2007, **126**, 272.

17 H. L. Chen, H. M. Lee, S. H. Chen and M. B. Chang, *Ind. Eng. Chem. Res.*, 2008, **47**, 2122.

18 C. H. Tsai, H. H. Yang, C. J. G. Jou and H. M. Lee, *J. Hazard. Mater.*, 2007, **143**, 409.

19 A. Mihalcioiu, K. Yoshida and M. Okubo, *IEEE T. Ind. Appl.*, 2010, **46**, 2151.

20 T. Kuroki, T. Fujioka, R. Kawabata and M. Okubo, *IEEE T. Ind. Appl.*, 2009, **45**, 10.

21. A. Ogata, D. Ito, K. Mizuno, S. Kushiyama, T. Yamamoto and S. Member, *IEEE T. Ind. Appl.*, 2001, **37**, 959.

22 Q. Yu, H. Wang, T. Liu, L. Xiao, X. Jiang and X. Zheng, *Environ. Sci. Technol.*, 2012, **46**, 2337.

23 F. Wang, X. L. Tang, H. H. Yi, K. Li, J. G. Wang and C. Wang, *RSC Adv.*, 2014, **4**, 8502.

24 X. L. Tang, F. Y. Gao, J. G. Wang, H. H. Yi, S. Z. Zhao, B. W. Zhang, Y. R. Zuo and Z. X. Wang, *Ind. Eng. Chem. Res.* 2014, **53**, 6197.

25 I. Jogi, V. Bichevin, M. Laan, A. Haljaste and H. Kaambre, *Plasma Chem. Plasma Process.*, 2009, **29**, 205.

26 S. Z. Zhao, H. H. Yi, X. L. Tang, F. Y. Gao, B. W. Zhang, Z. X. Wang, and Y. R. Zuo, *J. Clean. Prod.*, 2014, DOI: 10.1016/j.jclepro.2014.10.001.

27 H. H. Yi, H. Deng, X. L. Tang, Q. F. Yu, X. Zhou, and H. Y. Liu, *J. Hazard. Mater.*, 2012, **203-204**, 111.

28 H. L. Chen, H. M. Lee, S. H. Chen, M. B. Chang, S. J. Yu and S. N. Li, *Environ. Sci. Technol.*, 2009, **43**, 2216.

29 N. Xing, X. P. Wang, Q. Yu, X. W. Guo, *Chin. J. Catal.*, 2007, **28**, 205.

30 T. T. Yang, H. T. Bi, X. X. Cheng, *Appl. Catal. B*, 2011, **102**, 163.

31 I. Sobczak, K. Musialska, H. Pawlowski, M. Ziolek, *Catal. Today*, 2011, **176**, 393.

32 D. Eichwald, M. Yousfi, A. Hennad, and M. D. Benabdessadok, *J. Appl. Phys.*, 1997, **82**, 4781.

33 R. Atkinson, D. L. Baulch, R. A. Cox, R. F. Hampson Jr, J. A. Kerr, and J. Troe, Int. *J. Chem. Kinet.*, 1989, **21**, 115.

34 H. Sadat, N. Dubus, V. L. Dez, J. M. Tatibouët and J. Barrault, *J. Electrost.*, 2010, **68**, 27.

35 H. Sadat, N. Dubus, L. Pinard, J. M. Tatibouet, J. Barrault, *Appl. Therm. Eng.*, 2009, **29**, 1259.

36 P. C. Cosby, *J. Chem. Phys.*, 1993, **98**, 9544.

37 C. W. Walter, P. C. Cosby and H. Helm, *J. Chem. Phys.*, 1993, **90**, 3553.

38 G. B. Zhao, X. D. Hu, M. D. Argyle and M. N. Radosz, *Ind. Eng. Chem. Res.*, 2004, **43**, 5077.